

Using nanokelvin quantum thermometry to detect timelike Unruh effect in a Bose-Einstein condensate

Zehua Tian^{1,2,*} and Jiliang Jing³

¹*CAS Key Laboratory of Microscale Magnetic Resonance and School of Physical Sciences, University of Science and Technology of China, Hefei 230026, China*

²*CAS Center for Excellence in Quantum Information and Quantum Physics, University of Science and Technology of China, Hefei 230026, China*

³*Department of Physics, Key Laboratory of Low Dimensional Quantum Structures and Quantum Control of Ministry of Education, and Synergetic Innovation Center for Quantum Effects and Applications, Hunan Normal University, Changsha, Hunan 410081, P. R. China*

It is found that the Unruh effect can not only arise out of the entanglement between two sets of modes spanning the left and right Rindler wedges, but also between modes spanning the future and past light cones. Furthermore, an inertial Unruh-DeWitt detector along a spacetime trajectory in one of these cones may exhibit the same thermal response to the vacuum as that of an accelerated detector confined in the Rindler wedge. This feature thus could be an alternative candidate to verify the “Unruh effect”, termed as the timelike Unruh effect correspondingly. In this paper we propose to detect the timelike Unruh effect by using an impurity immersed in a Bose-Einstein condensate (BEC). The impurity acts as the detector which interacts with the density fluctuations in the condensate, working as an effective quantum field. Following the paradigm of the emerging field of *quantum thermometry*, we combine quantum parameter estimation theory with the theory of open quantum systems to realize a nondemolition Unruh temperature measurement in the nanokelvin (nK) regime. Our results demonstrate that the timelike Unruh effect can be probed using a stationary two-level impurity with time-dependent energy gap immersed in a BEC within current technologies.

I. INTRODUCTION

The Unruh effect [1] is a conceptually subtle quantum field theory result in relativistic framework. It plays a crucial role in our understanding that vacuum fluctuations and the particle content of a field theory are observer-dependent. It predicts that uniformly accelerating observers perceive the quantum field vacuum defined by inertial observers as a thermal state, rather than a zero-particle state. Since, to produce an experimentally appreciable Unruh temperature, prohibitively large accelerations have to be required (e.g., about 1 Kelvin even for accelerations as high as 10^{20} m/s²), the direct experimental confirmation of the Unruh effect until now still remains elusive.

A uniformly accelerating observer is conveniently described as a stationary observer in Rindler coordinates [2, 3]. From the perspective of the accelerating observer, the Minkowski vacuum state of a quantum field, e.g., a massless scalar field, defined by the inertial observers can be written as a spacelike entangled state between two sets of modes, respectively, spanning the left and right Rindler wedges [4]. Since the accelerating observer is confined to just one of these wedges, the thermalized vacuum is obtained (i.e., Unruh effect arises as the re-

sult of the spacelike entanglement) when tracing out the unobserved modes. To detect the Unruh effect, many experimental scenarios have been designed in the *analogue gravity* [5] regime, including various physical systems ranging from ultracold atoms systems [6–13] to a graphene nanosheet system [14]. In this regard, let us note that quantum simulation of Unruh effect has been reported through the BEC system [11] and NMR system [15] experimentally. These simulations rely on functional equivalence (i.e., simulating two-mode squeezed mechanics), while one significant step forward is to embody the essential of Unruh effect—*acceleration-induced* particle creation—in the simulation. Furthermore, other scenarios to enhance the detection of the acceleration-induced emission has been successfully theoretically put forward [16–20]. However, the intractable, but required, relativistic motion is still the main obstacle to verifying the Unruh effect in practice.

Recently, it has been shown that the Minkowski vacuum state of a quantum field could also be written down similarly as entangled states between modes spanning in the future and past light cones [21–23]. The Unruh effect may also arise as a result of this timelike entanglement if an observer (or detector interacting with the field) is confined only in one of these cones. In this case, a detector in the future/past light cone with world line $(\tau, 0)$ (see Fig. 1) corresponds to a detector with energy gap scaled with $1/at$ in the laboratory frame (see more details be-

* tianzh@ustc.edu.cn

low). Therefore, one can in principle detect this timelike Unruh effect by considering a stationary detector with a special form of time-dependent energy gap [21], while without involving any real relativistic motion. Note that extraction of timelike entanglement from the quantum vacuum [24] has been investigated with this model. Besides, Berry phase from the entanglement of future and past light cones has been proposed to detect this timelike Unruh effect [25]. However, a concrete experimentally feasible scenario to estimate the timelike Unruh effect is still lacking.

In this paper, we aim at resolving this issue by proposing to detect the timelike Unruh effect with an experimentally accessible platform consisting of a BEC and an immersed impurity [26, 27]. In our scenario, the density fluctuations in the BEC are modeled as the quantum field. The impurity, analogously dipole coupled to the density fluctuations, acts as an Unruh-DeWitt detector, and its energy gap can be designed as a time-dependent one by an external electromagnetic field (see more details below). We treat the impurity as an open system and derive its dynamical evolution by tracing over the degree of freedom of the analogous quantum field. Adopting tools from the theory of quantum parameter estimation, we show that our proposed scheme achieves experimentally accessible precision for the Unruh temperature detection in the BEC system within current technologies.

The outline of this paper is as follows. In Sec. II we review some basic concepts and physics of the Unruh effect from the perspective of quantum field theory and Unruh-DeWitt detector approach. In Sec. III we propose a concrete scenario to realize the detection of the timelike Unruh effect using the BEC platform. Experimental feasibility of the relevant analysis within the current technologies of BEC is discussed in Sec. IV. Finally, discussion and summary of the main results are present in Sec. V.

II. TIMELIKE UNRUH EFFECT

In this section we will simply review the timelike Unruh effect from the perspective of quantum field vacuum state and Unruh-DeWitt detector response. For more details, we refer the reader to Refs. [4, 21].

A. Quantum field vacuum state

Let us begin with the spacetime broken into quadrants (F, P, R, L) shown in Fig. 1. The corresponding four coordinate systems can be used to define a set of field modes, complete in each region. To derive the Unruh

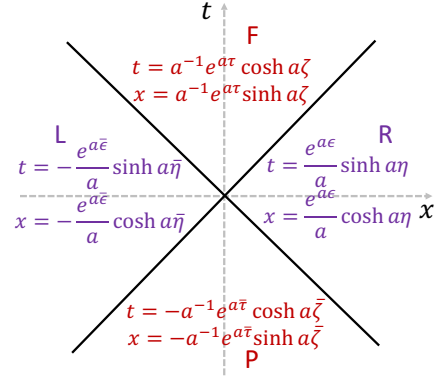


FIG. 1. A spacetime diagram divided into four quadrants: the future (F) and past (P) light cones, and the left (L) and right (R) Rindler wedges. The transform between the usual Minkowski coordinate (t, x) and that of the four regimes are shown. From the perspective of an accelerating observer, the Minkowski vacuum of massless quantum field can be expanded in terms of modes confined in R and L or in terms of modes restricted to F and P. Therefore, if the observer in one of these quadrants (e.g., the F light cone), tracing over the unobserved modes (e.g., in the P light cone) leads to the (timelike) Unruh effect.

effect, we here, for simplification, consider a two dimensional massless scalar field case for the example. Because of the conformal invariance of the massless wave equation in two dimensions, all the Klein-Gordon equations in the four coordinate systems are the same as that of two-dimensional Minkowski case. They are given by [4],

$$\left(\frac{\partial^2}{\partial \tau^2} - \frac{\partial^2}{\partial \zeta^2} \right)_F \phi = 0, \quad \left(\frac{\partial^2}{\partial \eta^2} - \frac{\partial^2}{\partial \epsilon^2} \right)_R \phi = 0, \quad (1)$$

$$\left(\frac{\partial^2}{\partial \bar{\tau}^2} - \frac{\partial^2}{\partial \bar{\zeta}^2} \right)_P \phi = 0, \quad \left(\frac{\partial^2}{\partial \bar{\eta}^2} - \frac{\partial^2}{\partial \bar{\epsilon}^2} \right)_L \phi = 0, \quad (2)$$

where the subscripts (F, P, R, L) denote the regions. Correspondingly, the set of field modes defined in the respective quadrants are given by

$$\phi_\omega^R(\chi) = (4\pi\omega)^{-1/2} e^{-i\omega\chi}, \quad \phi_\omega^L(\bar{\chi}) = (4\pi\omega)^{-1/2} e^{-i\omega\bar{\chi}}$$

$$\phi_\omega^F(\nu) = (4\pi\omega)^{-1/2} e^{-i\omega\nu}, \quad \phi_\omega^P(\bar{\nu}) = (4\pi\omega)^{-1/2} e^{-i\omega\bar{\nu}}$$

where $\chi = \eta + \epsilon$, $\bar{\chi} = -\bar{\eta} - \bar{\epsilon}$, $\nu = \tau + \zeta$, and $\bar{\nu} = -\bar{\tau} - \bar{\zeta}$ denote the “light-cone” in the four coordinate systems above.

One can quantize the field and define the field vacuum and field creation/annihilation operators in the respective quadrants. For example, one can define the Rindler vacuum as $\hat{a}_\omega^R|0_R\rangle = 0$ with \hat{a}_ω^R being the annihilation operator for a right Rindler particle, corresponding to the solution $\phi_\omega^R(\chi)$. Here ω here is the particle frequency. The particle number state is given by $\frac{(\hat{a}_\omega^{R\dagger})^n}{n!}|0_R\rangle = |n_\omega, R\rangle$ with $\hat{a}_\omega^{R\dagger}$ being the creation operator.

From the perspective of an accelerated observer, the vacuum of quantum massless scalar field, $|0_M\rangle$, defined by an inertial observer in the Minkowski spacetime can be rewritten as an entangled state between two sets of modes, respectively, spanning the right and left Rindler wedges [1, 4]:

$$|0_M\rangle = \prod_{i=1} \left(C_i \sum_{n_i=0}^{\infty} e^{-\pi n_i \omega_i / a} |n_i, R\rangle \otimes |n_i, L\rangle \right), \quad (5)$$

where $C_i = \sqrt{1 - e^{-2\pi\omega_i/a}}$, and n_i and ω_i respectively denote the Rindler particle number and energy in corresponding regions, R and L. However, since the R region and L region are causally disconnected (spacelike), the uniformly accelerated observer can only access one set of Rindler modes. The tracing out of the unobserved modes (e.g., the left Rindler modes) leads to the prediction that such an accelerated observer sees a thermalized vacuum, i.e.,

$$\hat{\rho}_R = \prod_{i=1} \left(C_i^2 \sum_{n_i=0}^{\infty} e^{-2\pi n_i \omega_i / a} |n_i, R\rangle \langle n_i, R| \right). \quad (6)$$

Note that this is density matrix for the system of free bosons with temperature $T = a/2\pi$. It means that the Minkowski vacuum state $|0_M\rangle$ of quantum field is viewed as a thermal state from the perspective of the accelerated observer, known as the Unruh effect.

Modes in R is independent from modes in L , and modes in F is independent from modes in P , but modes in F/P are not independent of the modes in R/L [21]. Actually, $\phi_\omega^F(\nu)$ is the same solution as $\phi_\omega^R(\chi)$, extended from R into F , which is pointed out in Refs. [4, 21]. This is also hold for $\phi_\omega^P(\nu)$ and $\phi_\omega^L(\chi)$. Therefore, the demonstration of F-P entanglement of the Minkowski vacuum is exactly the same as the standard demonstration of R-L entanglement shown in Eq. (5), with a change of labels $R \rightarrow F$ and $L \rightarrow P$. That is to say, the Minkowski vacuum restricted to $F - P$ takes a symmetrical form when expressed in terms of the “conformal modes” ϕ_ω^F and ϕ_ω^P :

$$|0_M\rangle = \prod_{i=1} \left(C_i \sum_{n_i=0}^{\infty} e^{-\pi n_i \omega_i / a} |n_i, F\rangle \otimes |n_i, P\rangle \right). \quad (7)$$

Analogously, the state of the field in the future (or the past) alone is a “thermal” state of the ϕ_ω^F (ϕ_ω^P)-modes, given by

$$\hat{\rho}_F = \prod_{i=1} \left(C_i^2 \sum_{n_i=0}^{\infty} e^{-2\pi n_i \omega_i / a} |n_i, F\rangle \langle n_i, F| \right). \quad (8)$$

Note that this thermal phenomenon in (8) arises out of the timelike entanglement between modes of F and P light cones, so it is also called as the timelike Unruh effect [21, 24].

B. Unruh-DeWitt detector response function

To detect the timelike Unruh effect, one can consider an Unruh-DeWitt detector evolving in the F light cone with world line $x = y = z = 0, t = a^{-1}e^{a\tau}$. Along this world line the Schrödinger equation in the conformal time τ reads $i\partial\psi/\partial\tau = H\psi$, and the eigenvalues of H is assumed to be a constant gap ω_0 . In Minkowski coordinates or laboratory framework, this Schrödinger equation can be rewritten as

$$i\frac{\partial\psi}{\partial t} = \frac{H}{at}\psi. \quad (9)$$

The $1/at$ factor is due to the change of variables to Minkowski time. This means that in the laboratory a detector with energy gap (denoted by the Hamiltonian H) scaled with $1/at$ corresponds to a detector with the fixed Hamiltonian H on the $x = y = z = 0, t = a^{-1}e^{a\tau}$ world line [21].

We can assume the interaction between the detector and the field to be the standard Unruh-DeWitt term. Specifically, for a two-level detector it takes the form $H_I = \lambda\hat{\phi}(x(t))\sigma_x$. Therefore, consider the full Hamiltonian in the conformal time framework, we have $i\partial\psi/\partial\tau = (H + e^{a\tau}H_I)\psi$. The interaction term acquires the exponential factor due to the change of variables to conformal time. For this case, the detector response function is found to be

$$\mathcal{G}(\omega_0) = \int_{-\infty}^{\infty} d\tau \int_{-\infty}^{\infty} d\tau' e^{-i\omega_0(\tau-\tau')} e^{a(\tau+\tau')} D^+(\tau, \tau') \quad (10)$$

where $D^+(\tau, \tau') = \langle 0_M | \phi(\tau)\phi(\tau') | 0_M \rangle$ denotes the Wightman function of the field. The Wightman function along the inertial trajectory $x = y = z = 0, t = a^{-1}e^{a\tau}$ can be calculated to take the form [21, 24]

$$D^+(\tau, \tau') = -\frac{a^2 e^{-a(\tau+\tau')}}{16\pi^2 \sinh^2 \left[\frac{a}{2}(\tau - \tau') - i\varepsilon \right]}, \quad (11)$$

while it along a uniformly accelerated trajectory $t = a^{-1} \sinh(a\eta), x = a^{-1} \cosh(a\eta), y = z = 0$ in the R region takes the form

$$D^+(\eta, \eta') = -\frac{a^2}{16\pi^2 \sinh^2 \left[\frac{a}{2}(\eta - \eta') - i\varepsilon \right]}. \quad (12)$$

With the Wightman functions in Eqs. (11) and (12), we can find the response function integral for the inertial detector in F region is formally identical to that for the accelerated detector in the R region. Furthermore, through the standard evaluation of the response function integral [3], this leads us to a thermal response function at temperature $T = \frac{a}{2\pi}$, called as the Unruh temperature. Note that the accelerated detector in R region can

demonstrate the Unruh effect in terms of its response function. However, the inertial detector in F region may also demonstrate the Unruh effect, while without involving any acceleration motion. Instead of that, it requires its energy gap scaled with $1/at$ in the laboratory [21, 24].

III. DETECT THE TIMELIKE UNRUH EFFECT IN A BEC

We will in the following observe the timelike Unruh effect with an impurity immersed into a BEC, and adopt tools from the theory of quantum parameter estimation to estimate the Unruh temperature.

A. Dynamics of the impurity detector in a BEC

To demonstrate the timelike Unruh effect with the Unruh-DeWitt detector model in a BEC, let us begin with the standard one-dimensional Gross-Pitaevskii equation [28–30]

$$i\partial_t\Psi = \left[-\frac{1}{2m}\nabla^2 + V_{\text{ext}} + g|\Psi|^2 \right]\Psi, \quad (13)$$

where Ψ is the condensate wave function, V_{ext} is the externally imposed trapping potential, and g denotes the two-body contact interaction coupling. In the second-quantized formalism, one can decompose the field operator for the dilute Bose gas as $\hat{\Psi} = \Psi_0(1 + \hat{\phi})$ with $\Psi_0 = \sqrt{\rho_0}e^{i\theta_0}$, where $|\Psi_0(x)|^2 = \rho_0 \simeq \text{const}$ represents the condensate density, and $\hat{\phi}$ describes the perturbations (excitations) on the top of the condensate. Within the Bogoliubov theory [31, 32], density fluctuations in Heisenberg representation can be written in the form of $\hat{\phi}$ as

$$\begin{aligned} \delta\hat{\rho}(t, x) &\simeq \rho_0(\hat{\phi} + \hat{\phi}^\dagger) = \sqrt{\rho_0} \int \frac{dk}{2\pi} (u_k + v_k) \\ &\times [\hat{b}_k e^{-i\omega_k t + ikx} + \hat{b}_k^\dagger e^{i\omega_k t - ikx}], \end{aligned} \quad (14)$$

which closely resembles the quantized scalar field in terms of bosonic operators \hat{b}_k (\hat{b}_k^\dagger) satisfying the usual Bose commutation rules $[\hat{b}_k, \hat{b}_{k'}^\dagger] = 2\pi\delta(k - k')$. In the laboratory frame where the condensate is at rest, the frequency of quasiparticle reads $\omega_k = c_0 k \sqrt{1 + (\xi_0 k/2)^2}$ with c_0 and ξ_0 being the speed of sound and the healing length, respectively. Note that u_k and v_k are Bogoliubov parameters satisfying $(u_k + v_k)^2 = E_k/\omega_k$ with $E_k = k^2/2m$.

We consider an impurity as the simulator of the Unruh-DeWitt detector, which is immersed into the condensate and collisionally coupled to the Bose gas. The impurity is assumed to be illuminated by a monochromatic external

electromagnetic field at the frequency close to resonance with the impurity's internal level transition, with a time-dependent Rabi frequency. The effective Hamiltonian of the whole system, the impurity plus the density fluctuations, is given by (see Supplemental Material [33] for details)

$$H(t) = \frac{\omega_0(t)}{2}\sigma_z + g_- \sigma_x \delta\hat{\rho}(x_A, t), \quad (15)$$

where $\omega_0(t)$ is the time-dependent Rabi frequency which can be experimentally controlled, and g_- is the coupling parameter. Therefore, the dynamics of this system yields $i\partial_t|\Psi\rangle = H(t)|\Psi\rangle = [\frac{\omega_0(t)}{2}\sigma_z + g_- \sigma_x \delta\hat{\rho}(x_A, t)]|\Psi\rangle$. If we introduce a new time parameter τ satisfying $t = c_0 a^{-1} e^{a\tau/c_0}$, then in this time frame one can find

$$i\partial_\tau|\Psi\rangle = [\frac{\omega_0}{2}\sigma_z + e^{a\tau/c_0} g_- \sigma_x \delta\hat{\rho}(x_A(\tau), t(\tau))]| \Psi\rangle, \quad (16)$$

where $\omega_0(t) = c_0 \omega_0 / at$ has been taken. This choice means that a two-level detector with energy gap scaled with c_0/at corresponds to a two-level detector with fixed energy gap ω_0 in the time τ frame. Note that this scenario also corresponds to a two-level detector with the fixed energy gap ω_0 on the $(\tau, 0)$ world line, which has been proposed to detect the timelike Unruh effect [21, 24, 25].

The correlation function of the density fluctuations with respect to the laboratory time t along the world line $(\tau, 0)$ reads (see Supplemental Material [33] for details)

$$\begin{aligned} \langle \delta\hat{\rho}(t(\tau)) \delta\hat{\rho}(t'(\tau')) \rangle &= -\frac{\rho_0}{4\pi m c_0} \frac{1}{(c_0 \Delta t - i\epsilon)^2} \\ &= \frac{-\rho_0 a^2}{16\pi m c_0^5} \frac{e^{-a(\tau+\tau')/c_0}}{\sinh^2[\frac{a}{2c_0} \Delta\tau - i\epsilon]} \end{aligned} \quad (17)$$

where $\Delta\tau = \tau - \tau'$ and $\langle \bullet \rangle = \langle 0 | \bullet | 0 \rangle$. With this, one can calculate the detector's response function as

$$\begin{aligned} \mathcal{G}(\omega_0) &= g_-^2 \int_{-\infty}^{\infty} d(\Delta\tau) e^{-i\omega_0 \Delta\tau} e^{\frac{a}{c_0}(\tau+\tau')} \langle \delta\hat{\rho}(\tau) \delta\hat{\rho}(\tau') \rangle \\ &= \Gamma(\omega_0) \frac{1}{e^{\frac{2\pi\omega_0 c_0}{a}} - 1}, \end{aligned} \quad (18)$$

where $\Gamma(\omega_0) = (\rho_0 \omega_0 g_-^2)/(2m c_0^3)$ is the spontaneous emission rate. Note that this response function is similar to that of the uniformly accelerating Unruh-DeWitt detector in R region [3]. As such, this thermal response implies that the detector views the vacuum fluctuations as a thermal bath with temperature $T = |a|/2\pi$. The timelike Unruh effect is thus demonstrated. To further explore this effect, we will explore the quantum dynamics of the impurity, and estimate the Unruh temperature with the quantum metrology approach below.

Since we are interested in the dynamics of the impurity, we trace over the degree of freedom of the analogue

quantum field. Besides, we perform the Born approximation and the Markov approximation as a results of the weak coupling between the impurity and field. We thus can find from Eq. (16), the dynamics evolution of the impurity is given by the Lindblad master equation

$$\dot{\rho}_A(\tau) = -i\Omega[\sigma_z, \rho_A(\tau)] + \mathcal{G}(\omega_0)\mathcal{L}[\sigma_+] + \mathcal{G}(-\omega_0)\mathcal{L}[\sigma_-], \quad (19)$$

where $\mathcal{L}(O) = O\rho O^\dagger - O^\dagger O\rho - \rho O^\dagger O$. Note that $\rho_A(\tau)$ is the time-dependent state of the impurity, and $\Omega = \omega_0 + \omega_L$ with ω_L being the Lamb shift [34] as a result of the interaction with vacuum fluctuations. Specifically, it reads

$$\omega_L = \frac{i}{2}[\mathcal{K}(-\omega_0) - \mathcal{K}(\omega_0)], \quad (20)$$

with $\mathcal{K}(\omega_0) = P \frac{1}{i\pi} \int_{-\infty}^{\infty} d\omega \frac{\mathcal{G}(\omega)}{\omega - \omega_0}$. Note that P denotes principle value. Because of $\Gamma(\omega_0)/\omega_0 \ll 1$, the Lamb shift is quite small and thus usually is assumed to be negligible.

Assuming the initial state of the impurity is prepared at $|\psi(0)\rangle = \sin(\theta/2)|g\rangle + \cos(\theta/2)e^{-i\phi}|e\rangle$, one can find the solution to Eq. (19) is $\rho_A(\tau) = \frac{1}{2}(\mathbf{I} + \boldsymbol{\omega}(\tau) \cdot \boldsymbol{\sigma})$ with

$$\begin{aligned} \omega_1 &= \sin\theta \cos(\Omega\tau + \phi)e^{-2\delta_+\tau}, \\ \omega_2 &= \sin\theta \sin(\Omega\tau + \phi)e^{-2\delta_+\tau}, \\ \omega_3 &= \cos\theta e^{-4\delta_+\tau} + \frac{\delta_-}{\delta_+}(1 - e^{-4\delta_+\tau}), \end{aligned} \quad (21)$$

where $\delta_{\pm} = \frac{1}{4}[\mathcal{G}(\omega_0) \pm \mathcal{G}(-\omega_0)]$, $\boldsymbol{\omega}(\tau) = (\omega_1(\tau), \omega_2(\tau), \omega_3(\tau))$, and $\boldsymbol{\sigma} = (\sigma_1, \sigma_2, \sigma_3)$ are Pauli matrixes. In the long evolution time limit, $\delta_+\tau \gg 1$, the impurity eventually evolves to the state

$$\rho_A(\infty) = \frac{e^{\beta H_0}}{\text{Tr}[e^{\beta H_0}]}, \quad (22)$$

regardless of the initial state. Here $H_0 = \frac{\omega_0}{2}\sigma_z$, and $\beta = 1/T$ denotes the inverse Unruh temperature. It means that the Unruh effect can be understood as a manifestation of thermalization phenomena that involves decoherence and dissipation in open quantum systems [35].

With the evolving state of the detector in Eq. (21), in the following we will estimate the Unruh temperature through quantum metrology approach, similar to our previous studies [36, 37].

B. Optimal estimation of the Unruh effect

As shown above we have proved that the impurity with a specially scaled energy gap may be exploited to observe the timelike Unruh effect in BEC. The Unruh temperature of the density fluctuations of BEC, viewed by

the impurity probe, parametrizes the probe state $\rho_A(\tau)$ shown in Eq. (21). Since the dependence of $\boldsymbol{\omega}(\tau)$ on T is well understood, one can infer this temperature from the statistics of measurements which are made on a large ensemble of identically prepared probes. However, as a result of the random character of quantum measurement and the finite size of the ensemble, uncertainty is unavoidable in any such temperature estimate. In this regard, the theory of quantum parameter estimation plays a crucial role in finding the optimal measurement that minimizes this uncertainty [38, 39].

In general, the solution of parameter estimation problem is to find an estimator which denotes a mapping $\hat{T} = \hat{T}(x_1, x_2, \dots)$ from the set of measurement outcomes into the space of parameters. Optimal estimators in classical estimation theory means that they can saturate the Cramér-Rao inequality [40, 41]

$$V(T) \geq \frac{1}{NF(T)}, \quad (23)$$

where N is the number of measurements, $F(T)$ is the so-called Fisher Information, and $V(T) = E_T[(\hat{T}(\{x\}) - T)^2]$ is the mean square error. This inequality establishes a lower bound on the mean square error of any estimator of the parameter T . Specifically, the Fisher Information

$$F(T) = \int dx p(x|T) \left(\frac{\partial \ln p(x|T)}{\partial T} \right)^2. \quad (24)$$

Here $p(x|T)$ denotes the conditional probability of obtaining the value x when the parameter has the value T . Furthermore, note that actually the mean square error is equal to the variance $\text{Var} = E_T[\hat{T}^2] - E_T[\hat{T}]^2$ for unbiased estimators.

In quantum version, the conditional probability according to the Born rule reads $p(x|T) = \text{Tr}[\Pi_x \rho_T]$, where $\{\Pi_x\}$ denotes a positive operator-valued measure satisfying $\int dx \Pi_x = \mathbf{I}$. Moreover, ρ_T is the density operator parametrized by the temperature T we want to estimate. By introducing the Symmetric Logarithmic Derivative (SLD) \hat{L}_T as the self-adjoint operator satisfying

$$\frac{\hat{L}_T \rho_T + \rho_T \hat{L}_T}{2} = \frac{\partial \rho_T}{\partial T}, \quad (25)$$

the Fisher information (24) then can be rewritten as

$$F(T) = \int dx \frac{\Re(\text{Tr}[\rho_T \Pi_x \hat{L}_T])^2}{\text{Tr}[\rho_T \Pi_x]}. \quad (26)$$

Therefore, for a given quantum measurement, Eqs. (23) and (26) establish the classical bound on precision, which may be achieved by a proper data processing, e.g., by maximum likelihood, which is known to provide an

asymptotically efficient estimator. Since each measurement may have a corresponding Fisher information of its own, to find the ultimate bounds to precision one has to optimize the Fisher information over the quantum measurements. In this regard, the Fisher information $F(T)$ of any quantum measurements is bounded by the so-called Quantum Fisher Information (QFI), $F^Q(T) = \text{Tr}[\rho_T \hat{L}_T^2] = \text{Tr}[\partial_T \rho_T \hat{L}_T]$, which leads the Cramér-Rao bound of quantum version,

$$\text{Var}(T) \geq \frac{1}{NF(T)} \geq \frac{1}{NF^Q(T)}. \quad (27)$$

This inequality is valid for the variance of any estimator. We also define the quantum signal-to-noise ratio (QSNR) $Q^2 = T^2 F^Q(T)$, which bounds the signal-to-noise ratio as $T/\Delta T \leq \sqrt{NQ}$. Hence, Q here can be used to quantify the ultimate sensitivity limit of our impurity thermometer.

For a qubit probe, the QFI has a simple expression in terms of the Bloch vector [42]. Applying that to our Unruh-DeWitt detector case shown in (21), we can obtain

$$F^Q(T) = \begin{cases} \frac{(\omega \cdot \partial_T \omega)^2}{1 - |\omega|^2} + |\partial_T \omega|^2, & \omega < 1, \\ |\partial_T \omega|^2, & \omega = 1. \end{cases} \quad (28)$$

Note that the QFI for the mixed states cases (the first line of Eq. (28)) can be rewritten as

$$F^Q(T) = \frac{(\partial_T \lambda_+)^2}{\lambda_+} + \frac{(\partial_T \lambda_-)^2}{\lambda_-}, \quad (29)$$

where $\lambda_{\pm} = (1 \pm |\omega|)/2$ are two eigenvalues of the density operator of the qubit state. The corresponding eigenstates are

$$|p_+(\tau)\rangle = \sin \frac{\theta(\tau)}{2} |g\rangle + e^{-i\Omega\tau - i\phi} \cos \frac{\theta(\tau)}{2} |e\rangle, \quad (30)$$

$$|p_-(\tau)\rangle = \cos \frac{\theta(\tau)}{2} |g\rangle - e^{-i\Omega\tau - i\phi} \sin \frac{\theta(\tau)}{2} |e\rangle, \quad (31)$$

with

$$\tan \frac{\theta(\tau)}{2} = \sqrt{\frac{|\omega| - \omega_3}{|\omega| + \omega_3}}. \quad (32)$$

Eq. (29) means that the QFI in (28) consists of two terms, respectively corresponding to the Fisher information for measurements of $|p_+(\tau)\rangle\langle p_+(\tau)|$ and $|p_-(\tau)\rangle\langle p_-(\tau)|$. The SLD is given by

$$\hat{L}_T = \cos \varphi |p_+(\tau)\rangle\langle p_+(\tau)| + \sin \varphi |p_-(\tau)\rangle\langle p_-(\tau)|, \quad (33)$$

with

$$\tan \varphi = \frac{\lambda_+ \partial_T \lambda_-}{\lambda_- \partial_T \lambda_+}. \quad (34)$$

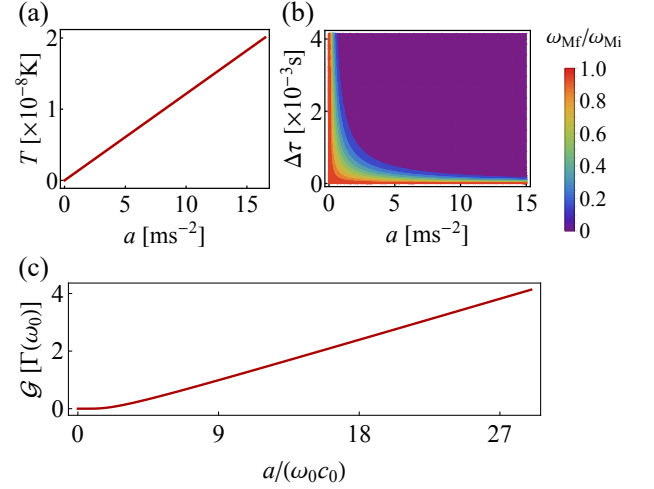


FIG. 2. (a) The temperature of the timelike Unruh effect via the effective acceleration; (b) the ratio of the initial, ω_{Mi} and final, ω_{Mf} , frequencies in the laboratory frame as a function of the effective acceleration and the conformal evolution time of the detector; (c) the detector's response function (in the units of detector's spontaneous emission rate $\Gamma(\omega_0)$) as a function of the dimensionless acceleration parameter. Here we take a typical value for the speed of sound in the condensate $c_0 \sim 10^{-3} \text{ m/s}$.

Since the SLD is directly related to the QFI and optimizes the quantum Cramér-Rao bound, measuring \hat{L}_T means to minimize the uncertainty in the Unruh temperature estimate due to the finite number of samples. Furthermore, it is needed to point out that the SLD depends on the temperature, and thus some prior information on T is assumed when constructing its corresponding measurement. Seen from the expression of the SLD in Eq. (33), if one wants to measure \hat{L}_T in practice, then one is required to be able to efficiently evaluate the Bloch vector $\omega(\tau)$ and its temperature derivatives from an accurate theoretical model for the detector's state $\rho_A(\tau)$. In addition, the ability to measure an arbitrary combination of $\Pi_+ = \frac{1+\mathbf{n}\cdot\boldsymbol{\sigma}}{2}$ and $\Pi_- = \frac{1-\mathbf{n}\cdot\boldsymbol{\sigma}}{2}$ is also needed.

IV. EXPERIMENTAL IMPLEMENTATION

Recent experimental advances have allowed for groundbreaking observations of BEC, its excitation spectrum, and dynamics of impurity immersed in the BEC [43–45]. These relevant technologies in principle hold promise to realize our experimental scenario about timelike Unruh effect proposed above. We here make an estimate of the experimental parameters that are required to observe single-detector thermalization resulting from the timelike Unruh effect.

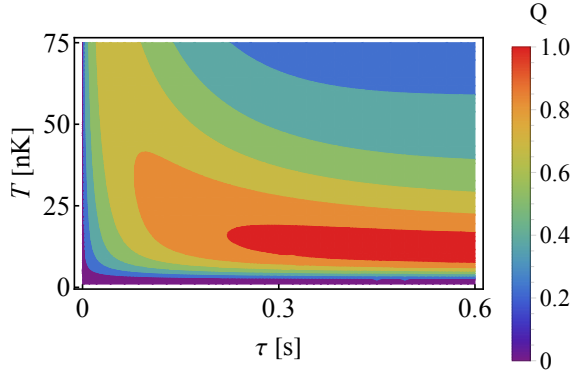


FIG. 3. QSNR as a function of the Unruh temperature and the conformal evolution time of the detector for $\theta = \pi$ (i.e., the initial ground state). Here we take a typical value for the speed of sound in the condensate $c_0 \sim 10^{-3}$ m/s, the spontaneous emission rate $\Gamma(\omega_0)/\omega_0 \sim 10^{-3}$, and the fixed energy gap of the detector in conformal time framework $\omega_0 = 2\pi \times 500$ Hz.

A. Unruh temperature and the conformal evolution time

As shown above, a “conformal observer” (i.e., in the τ framework with constant conformal frequency gap) actually will see a constant temperature

$$T = \frac{\hbar a}{2\pi c_0 k_B}. \quad (35)$$

By taking typical value for the speed of sound in the condensate $c_0 \sim 10^{-3}$ m/s, the Unruh temperature via the effective acceleration a is shown in Fig. 2 (a). It is found that 1 K timelike Unruh temperature in the BEC approximately requires the effective acceleration as high as 10^8 m/s², which is quite smaller than that for the massless scalar field case, on the order of 10^{20} m/s². This is because that the massless scalar field (or electromagnetic field) usually considered to observe the Unruh effect is replaced with the phononic field here, and the corresponding sound speed to which is much smaller than the speed of light in the vacuum. However, for the perspective of scaling the detector energy gap, we find that this scaling a/c_0 plays the key role in the temperature (35), and 1 K Unruh temperature requires a scaling on the order of 100 GHz.

We now need to clarify the correspondence between these conformal parameters and the laboratory frame parameters (i.e., Minkowski time intervals and frequencies). In particular, the relation between the time interval of observation in the laboratory frame and that of the conformal time $\Delta\tau$ reads

$$\Delta t = \frac{c_0 \omega_0}{a \omega_{\text{Mi}}} \left(e^{\frac{a \Delta\tau}{c_0}} - 1 \right), \quad (36)$$

where ω_{Mi} denotes the initial frequency of the two-level Unruh-DeWitt detector in the laboratory frame. Usually, since in practice the change of the frequency is not arbitrary, the ratio of the initial, ω_{Mi} and final, ω_{Mf} , frequencies in the laboratory frame needs to be confined and clarified. This ratio is given by

$$\frac{\omega_{\text{Mf}}}{\omega_{\text{Mi}}} = e^{-a \Delta\tau / c_0}. \quad (37)$$

It means the conformal time interval $\Delta\tau$ is confined. However, it is pointed out in Ref. [46] that unlike the electromagnetic case, the Rabi frequency in our cold atom setup could be tuned to zero, which gives $\omega_0 = 0$. Therefore, here we won’t limit the ratio of the initial and final frequencies in the laboratory frame. We plot this ratio as a function of the effective acceleration and the conformal evolution time of the detector in Fig. 2 (b). To observe the timelike Unruh effect, the high enough effective acceleration is required to result in high enough temperature, and the long enough conformal evolution time $\Delta\tau$ of the detector is also needed to accumulate more effects on the detector (i.e., to thermalize the detector or to achieve the thermal equilibrium between the detector and the Unruh thermal bath). However, considering the practical limited time interval of observation in the laboratory frame, we should choose proper effective acceleration and the conformal evolution time because of Eq. (36). We will in the following analyze the thermometric performance with considering these conditions. Furthermore, in Fig. 2 (c) we plot the detector’s response function (or spontaneous excitation rate) as a function of the dimensionless acceleration parameter. With the increase of the acceleration, the spontaneous excitation rate increases monotonously. This function may be explored to verify the thermal character of the timelike Unruh effect.

B. Thermometric performance

Note that the thermometer which measures the temperature of a BEC in the sub-nK regime has been investigated recently [47–51]. We here consider the similar thermometer to estimate the Unruh temperature.

Fig. 3 shows the QSNR as a function of the Unruh temperature and the conformal evolution time of the detector for $\theta = \pi$ (i.e., the initial ground state). At a given temperature, the optimal measurement time corresponds to the maximum sensitivity, i.e., $Q_{\text{max}} = \max_{\tau} Q(\tau) = Q(\tau_{\text{max}})$. It would be a certain moment before the thermal equilibrium between the detector and the Unruh thermal bath, or the long evolution time limit, $\delta_+ \tau \gg 1$, (i.e., the thermal equilibrium case), which depends on the Unruh temperature. It is found that the

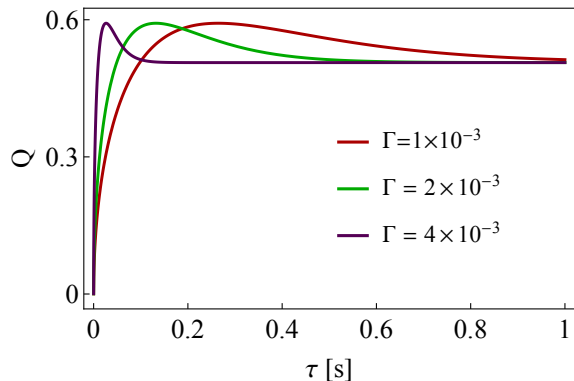


FIG. 4. QSNR at $T = 20$ nK as a function of the conformal evolution time of the detector for various $\Gamma = \Gamma(\omega_0)/\omega_0$ (which can be considered as the parameterized coupling strength) by taking $\theta = \pi$ (i.e., the initial ground state). Here we take a typical value for the speed of sound in the condensate $c_0 \sim 10^{-3}$ m/s, and the fixed energy gap of the detector in conformal time framework $\omega_0 = 2\pi \times 500$ Hz.

QSNR may achieve its maximum, shown as the large red region in Fig. 3, in the relevant temperature range which is valid within current experiments [52–54]. For example, if $T = 20$ nK we find $Q_{\max} \approx 0.59$, meaning that an error of $\Delta T/T \approx 10\%$ can be achieved with $N \approx 280$ measurements after a time $\Delta\tau_{\max} \approx 0.265$ s. According to Eq. (36), this conformal evolution time corresponds to an approximately infinite long laboratory time, i.e., $\Delta t \rightarrow \infty$. Therefore, the maximum sensitivity Q_{\max} seems not to be achieved. However, one can still achieve the same error by properly choosing the measurement time and the measurement number. For example, if $\Delta\tau = 0.55$ ms, and the measurement number $N = 50000$, one can achieve the error $\Delta T/T \approx 10\%$ with the laboratory time $\Delta t \approx 0.55$ s, which is eminently feasible since a single gas sample may have a lifetime of several seconds [55–57]. Furthermore, instead of looking at a single impurity, we can consider, say, 1000 to a few thousand of independent impurities [58, 59]. In this case, we can effectively reduce the measurement (e.g., to $N = 50$) while to achieve the same expected error $\Delta T/T \approx 10\%$.

The coupling strength between the detector and the field, which can be experimental controlled, plays an important role in the thermometric performance. In our model, the coupling strength can be embodied by the spontaneous emission rate $\Gamma(\omega_0)$ shown under Eq. (18). Therefore, different spontaneous emission rates could represent different coupling strength. In Fig. 4, we fix the Unruh temperature $T = 20$ nK and show the dynamical QSNR for various coupling strength. We find that the coupling strength does not affect the maximum sensitivity, while influences the optimal measurement time at which the maximum sensitivity can be achieved. The

maximum sensitivity shifts to progressively later times as the coupling strength decreases. As discussed above, it seems that the maximum sensitivity can not be obtained experimentally since the optimal measurement time in conformal frame usually might correspond to infinite time in the laboratory according to Eq. (36). Note that the correspondence between the conformal time and the laboratory time does not depend on the coupling strength. Therefore, although the experimentally feasible laboratory time (or the conformal evolution time) is fixed and usually smaller than the optimal measurement time, by controlling the coupling strength (i.e., increasing the coupling strength) one can still in principle obtain a considerable QSNR which approaches to the maximum sensitivity. For example, if we choose the laboratory time $\Delta t = 2$ s which is smaller than the lifetime of a single gas sample and thus is eminently experimentally feasible, then the corresponding conformal evolution time $\Delta\tau \approx 0.63$ ms, thus the corresponding QSNR $Q \approx 0.05, 0.07, 0.1$ for $\Gamma(\omega_0)/\omega_0 = 10^{-3}, 2 \times 10^{-3}, 4 \times 10^{-3}$ cases, respectively.

To further understand how the coupling strength affects the estimation of the Unruh temperature, in Fig. 5 (a) we fix an eminently experimentally feasible time $\Delta\tau \approx 0.63$ ms for the Unruh temperature $T = 20$ nK and show the relative error $\Delta T/T$ as a function of the effective coupling strength for different measurement number N . Remarkably, increasing the coupling strength can effectively reduce the error, meaning that the estimation of the Unruh temperature is more precise. For example, after 40000 measurements, the relative error for the $\Gamma(\omega_0)/\omega_0 = 0.2 \times 10^{-3}$ case is about 22.3%, while for the $\Gamma(\omega_0)/\omega_0 = 4 \times 10^{-3}$ case, this achieved relative error is around 5% and thus is effectively reduced. Furthermore, as shown in Fig. 5 (b) we can improve the estimation precision (or reduce the error) by increasing the measurements since $\Delta T/T \propto 1/\sqrt{N}$. However, on the other hand, the huge number of measurement may take a lot of time and lower the experimental efficiency. To achieve the same measurement error, the stronger coupling strength can effectively reduce the number of measurement under the same condition. For example, if our target error is around 10%, for the $\Gamma(\omega_0)/\omega_0 = 1 \times 10^{-3}$ case, the required measurements are about 39788, while for the $\Gamma(\omega_0)/\omega_0 = 4 \times 10^{-3}$ case, the required measurements are around 10028. In Fig. 5 (c) we fix an eminently experimentally feasible time $\Delta t = 4$ s and show the relative error $\Delta T/T$ as a function of the experimentally feasible Unruh temperature T in nK and even sub-nK regime. We find that in this case the relative error decreases with the increase of the Unruh temperature, meaning that we can obtain more precision when estimating the Unruh

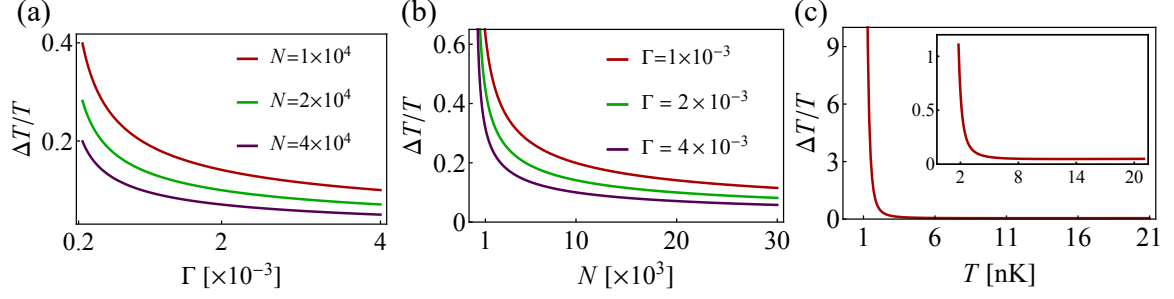


FIG. 5. (a) The relative error $\Delta T/T$ at $T = 20$ nK as a function of the spontaneous emission rate $\Gamma = \Gamma(\omega_0)/\omega_0$ (which can be considered as the parameterized coupling strength) for measurement number N by taking $\theta = \pi$ (i.e., the initial ground state); (b) the relative error $\Delta T/T$ at $T = 20$ nK as a function of the measurement number N for different spontaneous emission rates $\Gamma = \Gamma(\omega_0)/\omega_0$ by taking $\theta = \pi$ (i.e., the initial ground state); (c) the relative error $\Delta T/T$ at $\Gamma = 4 \times 10^{-3}$ and $N = 4 \times 10^4$ as a function of the experimentally feasible Unruh temperature T by taking $\theta = \pi$ (i.e., the initial ground state). Here we take a typical value for the speed of sound in the condensate $c_0 \sim 10^{-3}$ m/s, and the fixed energy gap of the detector in conformal time framework $\omega_0 = 2\pi \times 500$ Hz.

temperature in the relatively higher temperature regime.

V. DISCUSSIONS AND CONCLUSIONS

The parameters were chosen above just as an example that our proposed setup is feasible, which should not be considered as the only available configuration. Actually, we can also choose a higher effective acceleration a to create a higher temperature than nK. Repeat the same analysis, we can get the thermometric performance, going beyond the nK regime. Note that the main limited factor in our proposal is the time interval of observation in the laboratory frame since even the finite product of the acceleration and the conformal time, i.e., $a\Delta\tau$, may corresponds to a very huge laboratory time (see Eq. (36)), which can not be accessible experimentally. However, for a fixed $a\Delta\tau$, it is possible to choose the different combinations of the acceleration and the conformal evolution time to improve and optimize the performance of our proposal.

Usually the Unruh effect is notoriously difficult to observe, since the temperature is so tiny for accessible values of the acceleration, a , namely $T = \frac{\hbar a}{2\pi ck_B}$. In other words, to achieve an experimentally accessible Unruh temperature, quite high acceleration, which actually has been far beyond our ability, has to be required (e.g., 1K temperature requires about 10^{20} m/s² acceleration). Here we propose to detect the so-called timelike Unruh effect [21, 24, 25] in a BEC system. In our scenario, an inertial two-level detector, whose energy gap is continuously scaled as $1/at$ responds to the Minkowski vacuum in a manner identical to an accelerated detector with a fixed proper-energy gap. Instead of doing the real relativistic motion, e.g., quite high linear acceleration, we here

just need to control the time-dependent Rabi frequency of the detector, and thus it seems to be more accessible for experiment.

Thermalization is a key feature of Unruh effect. Thus, an important question arises: is the energy gap of the detector scaled over a long enough period to allow thermalization? Let us consider a detector in conformal time is scaled between times τ_1 and τ_2 , and assume that within the interaction time period many oscillations happens at the constant frequency (in the conformal time τ frame) ω_0 of the detector. This requirement means $\Delta\tau = \tau_2 - \tau_1 \gg \omega_0^{-1}$. In the laboratory frame, it corresponds to $\frac{t_2}{t_1} = e^{a\Delta\tau} \gg e^{a/\omega_0} = e^{1/(t_1\tilde{\omega}_1)} = e^{1/(t_2\tilde{\omega}_2)}$, where t_i and $\tilde{\omega}_i$ with $i = \{1, 2\}$ are respectively the laboratory time and the corresponding detector's energy gap at which. If $t_1 \approx 1/\tilde{\omega}_1$, then thermalization requires $t_2 \gg 2.71t_1$. In this regard, these thermalization conditions could lead us to choose certain appropriate experimental parameters to access to the optimal measurement time and thus realize the maximum sensitivity.

In our scheme, we estimate the Unruh temperature by monitoring the impurity atoms only, while without measuring the BEC itself destructively. Moreover, our scheme is inherently nonequilibrium and all the underlying analysis does not assume thermalization of the impurity at the temperature of the expected Unruh bath, thus alleviating the need for thermalization of the probe before accurate temperature estimation is feasible.

In summary, we present a concrete experimental proposal to detect the timelike Unruh effect that arises out of the entanglement between future and past light cones. Specifically, our model is based on an impurity with a time-dependent energy gap immersed in a BEC. We choose some typical experimentally accessible parameters to investigate the thermometric performance and

find very low relative error of the estimated Unruh temperature can be obtained. Therefore, the preliminary estimates indicate that the proposed experimental implementation of the timelike Unruh effect is within reach of current state-of-the-art ultracold-atom experiments.

Our proposed quantum fluid platform may also allow us in the experimentally accessible regime to explore interesting questions concerning extraction of time-like entanglement from the quantum field vacuum [24], Unruh effect induced geometric phase [17, 25], Lorentz-

invariance-violation-induced nonthermal Unruh effect [9], and so on.

ACKNOWLEDGMENTS

This work was supported by the National Natural Science Foundation of China under Grant No. 11905218, and the CAS Key Laboratory for Research in Galaxies and Cosmology, Chinese Academy of Science (No. 18010203).

-
- [1] W. G. Unruh, “Notes on black-hole evaporation,” *Phys. Rev. D* **14**, 870–892 (1976).
 - [2] W. Rindler, “Hyperbolic motion in curved space time,” *Phys. Rev.* **119**, 2082–2089 (1960).
 - [3] Nicholas David Birrell and PCW Davies, “Quantum fields in curved space,” Cambridge university press (1984).
 - [4] Luis C. B. Crispino, Atsushi Higuchi, and George E. A. Matsas, “The unruh effect and its applications,” *Rev. Mod. Phys.* **80**, 787–838 (2008).
 - [5] Carlos Barceló, Stefano Liberati, and Matt Visser, “Analogue gravity,” *Living Reviews in Relativity* **14**, 3 (2011).
 - [6] A. Retzker, J. I. Cirac, M. B. Plenio, and B. Reznik, “Methods for detecting acceleration radiation in a bose-einstein condensate,” *Phys. Rev. Lett.* **101**, 110402 (2008).
 - [7] Tianze Sheng, Jun Qian, Xiaolin Li, Yueping Niu, and Shangqing Gong, “Quantum simulation of the unruh effect with a rydberg-dressed bose-einstein condensate,” *Phys. Rev. A* **103**, 013301 (2021).
 - [8] Jamir Marino, Gabriel Menezes, and Iacopo Carusotto, “Zero-point excitation of a circularly moving detector in an atomic condensate and phonon laser dynamical instabilities,” *Phys. Rev. Research* **2**, 042009 (2020).
 - [9] Zehua Tian, Longhao Wu, Liang Zhang, Jiliang Jing, and Jiangfeng Du, “Probing lorentz-invariance-violation-induced nonthermal unruh effect in quasi-two-dimensional dipolar condensates,” *Phys. Rev. D* **106**, L061701 (2022).
 - [10] Cisco Gooding, Steffen Biermann, Sebastian Erne, Jorma Louko, William G. Unruh, Jörg Schmiedmayer, and Silke Weinfurter, “Interferometric unruh detectors for bose-einstein condensates,” *Phys. Rev. Lett.* **125**, 213603 (2020).
 - [11] Jiazhong Hu, Lei Feng, Zhendong Zhang, and Cheng Chin, “Quantum simulation of unruh radiation,” *Nature Physics* **15**, 785–789 (2019).
 - [12] W. G. Unruh, “Black holes, acceleration temperature and low temperature analog experiments,” *Journal of Low Temperature Physics* **208**, 196–209 (2022).
 - [13] Cameron R. D. Bunney, Steffen Biermann, Vitor S. Barroso, August Geelmuyden, Cisco Gooding, Grégoire Itier, Xavier Rojas, Jorma Louko, and Silke Weinfurter, “Third sound detectors in accelerated motion,” (2023), [arXiv:2302.12023 \[gr-qc\]](https://arxiv.org/abs/2302.12023).
 - [14] Xiaodong Zeng and M. Suhail Zubairy, “Graphene plasmon excitation with ground-state two-level quantum emitters,” *Phys. Rev. Lett.* **126**, 117401 (2021).
 - [15] FangZhou Jin, HongWei Chen, Xing Rong, Hui Zhou, MingJun Shi, Qi Zhang, ChenYong Ju, YiFu Cai, Shun-Long Luo, XinHua Peng, and JiangFeng Du, “Experimental simulation of the unruh effect on an nmr quantum simulator,” *Science China Physics, Mechanics & Astronomy* **59**, 630302 (2016).
 - [16] Marlan O. Scully, Vitaly V. Kocharovskiy, Alexey Belyanin, Edward Fry, and Federico Capasso, “Enhancing acceleration radiation from ground-state atoms via cavity quantum electrodynamics,” *Phys. Rev. Lett.* **91**, 243004 (2003).
 - [17] Eduardo Martín-Martínez, Ivette Fuentes, and Robert B. Mann, “Using berry’s phase to detect the unruh effect at lower accelerations,” *Phys. Rev. Lett.* **107**, 131301 (2011).
 - [18] Kinjalk Lochan, Hendrik Ulbricht, Andrea Vinante, and Sandeep K. Goyal, “Detecting acceleration-enhanced vacuum fluctuations with atoms inside a cavity,” *Phys. Rev. Lett.* **125**, 241301 (2020).
 - [19] Navdeep Arya, Vikash Mittal, Kinjalk Lochan, and Sandeep K. Goyal, “Geometric phase assisted observation of noninertial cavity-qed effects,” *Phys. Rev. D* **106**, 045011 (2022).
 - [20] D. Jaffino Stargen and Kinjalk Lochan, “Cavity optimization for unruh effect at small accelerations,” *Phys. Rev. Lett.* **129**, 111303 (2022).
 - [21] S. Jay Olson and Timothy C. Ralph, “Entanglement between the future and the past in the quantum vacuum,” *Phys. Rev. Lett.* **106**, 110404 (2011).
 - [22] Atsushi Higuchi, Satoshi Iso, Kazushige Ueda, and Kazuhiro Yamamoto, “Entanglement of the vacuum between left, right, future, and past: The origin of entanglement-induced quantum radiation,” *Phys. Rev. D* **96**, 083531 (2017).
 - [23] Kazushige Ueda, Atsushi Higuchi, Kazuhiro Yamamoto, Ar Rohim, and Yue Nan, “Entanglement of the vacuum between left, right, future, and past: Dirac spinor in rindler and kasner spaces,” *Phys. Rev. D* **103**, 125005 (2021).
 - [24] S. Jay Olson and Timothy C. Ralph, “Extraction of timelike entanglement from the quantum vacuum,” *Phys. Rev. A* **85**, 012306 (2012).
 - [25] James Q. Quach, Timothy C. Ralph, and William J. Munro, “Berry phase from the entanglement of future and past light cones: Detecting the timelike unruh effect,” *Phys. Rev. Lett.* **129**, 160401 (2022).

- [26] A. Recati, P. O. Fedichev, W. Zwerger, J. von Delft, and P. Zoller, “Atomic quantum dots coupled to a reservoir of a superfluid bose-einstein condensate,” *Phys. Rev. Lett.* **94**, 040404 (2005).
- [27] Petr O. Fedichev and Uwe R. Fischer, “Gibbons-hawking effect in the sonic de sitter space-time of an expanding bose-einstein-condensed gas,” *Phys. Rev. Lett.* **91**, 240407 (2003).
- [28] “Structure of a quantized vortex in boson systems,” *Il Nuovo Cimento* (1955-1965) **20**, 454–477 (1961).
- [29] Eugene P Gross, “Hydrodynamics of a superfluid condensate,” *Journal of Mathematical Physics* **4**, 195–207 (1963).
- [30] “Vortex lines in an imperfect bose gas,” *Sov. Phys. JETP* **13**, 451–454 (1961).
- [31] Christopher J Pethick and Henrik Smith, *Bose–Einstein condensation in dilute gases* (Cambridge university press, 2008).
- [32] Lev Petrovich Pitaevskii and Sandro Stringari, *Bose–Einstein Condensation and Superfluidity*, Vol. 164 (Oxford University Press, 2016).
- [33] *See Supplemental Material for details of calculations.*
- [34] Willis E. Lamb and Robert C. Retherford, “Fine structure of the hydrogen atom by a microwave method,” *Phys. Rev.* **72**, 241–243 (1947).
- [35] F. Benatti and R. Floreanini, “Entanglement generation in uniformly accelerating atoms: Reexamination of the unruh effect,” *Phys. Rev. A* **70**, 012112 (2004).
- [36] Zehua Tian, Jieci Wang, Heng Fan, and Jiliang Jing, “Relativistic quantum metrology in open system dynamics,” *Scientific Reports* **5**, 7946 (2015).
- [37] Jieci Wang, Zehua Tian, Jiliang Jing, and Heng Fan, “Quantum metrology and estimation of unruh effect,” *Scientific Reports* **4**, 7195 (2014).
- [38] MATTEO G. A. PARIS, “Quantum estimation for quantum technology,” *International Journal of Quantum Information* **07**, 125–137 (2009), <https://doi.org/10.1142/S0219749909004839>.
- [39] Mohammad Mehboudi, Anna Sanpera, and Luis A Correa, “Thermometry in the quantum regime: recent theoretical progress,” *Journal of Physics A: Mathematical and Theoretical* **52**, 303001 (2019).
- [40] Harald Cramér, *Mathematical Methods of Statistics*, Vol. 26 (Princeton University Press, 1999).
- [41] Samuel L. Braunstein and Carlton M. Caves, “Statistical distance and the geometry of quantum states,” *Phys. Rev. Lett.* **72**, 3439–3443 (1994).
- [42] Wei Zhong, Zhe Sun, Jian Ma, Xiaoguang Wang, and Franco Nori, “Fisher information under decoherence in bloch representation,” *Phys. Rev. A* **87**, 022337 (2013).
- [43] E. A. Cornell and C. E. Wieman, “Nobel lecture: Bose-einstein condensation in a dilute gas, the first 70 years and some recent experiments,” *Rev. Mod. Phys.* **74**, 875–893 (2002).
- [44] R. Ozeri, N. Katz, J. Steinhauer, and N. Davidson, “Colloquium: Bulk bogoliubov excitations in a bose-einstein condensate,” *Rev. Mod. Phys.* **77**, 187–205 (2005).
- [45] Michał Tomza, Krzysztof Jachymski, Rene Gerritsma, Antonio Negretti, Tommaso Calarco, Zbigniew Idziaszek, and Paul S. Julienne, “Cold hybrid ion-atom systems,” *Rev. Mod. Phys.* **91**, 035001 (2019).
- [46] Jamir Marino, Alessio Recati, and Iacopo Carusotto, “Casimir forces and quantum friction from ginzburg radiation in atomic bose-einstein condensates,” *Phys. Rev. Lett.* **118**, 045301 (2017).
- [47] Mohammad Mehboudi, Aniello Lampo, Christos Charalambous, Luis A. Correa, Miguel Ángel García-March, and Maciej Lewenstein, “Using polarons for sub-nk quantum nondemolition thermometry in a bose-einstein condensate,” *Phys. Rev. Lett.* **122**, 030403 (2019).
- [48] Rudolf Gati, Borge Hemmerling, Jonas Fölling, Michael Albiez, and Markus K. Oberthaler, “Noise thermometry with two weakly coupled bose-einstein condensates,” *Phys. Rev. Lett.* **96**, 130404 (2006).
- [49] Carlos Sabín, Angela White, Lucia Hackermuller, and Ivette Fuentes, “Impurities as a quantum thermometer for a bose-einstein condensate,” *Scientific Reports* **4**, 6436 (2014).
- [50] Muhammad Miskeen Khan, Mohammad Mehboudi, Hugo Terças, Maciej Lewenstein, and Miguel Angel Garcia-March, “Subnanokelvin thermometry of an interacting d -dimensional homogeneous bose gas,” *Phys. Rev. Res.* **4**, 023191 (2022).
- [51] Mark T. Mitchison, Thomás Fogarty, Giacomo Guarneri, Steve Campbell, Thomas Busch, and John Goold, “In situ thermometry of a cold fermi gas via dephasing impurities,” *Phys. Rev. Lett.* **125**, 080402 (2020).
- [52] A. E. Leanhardt, T. A. Pasquini, M. Saba, A. Schirotzek, Y. Shin, D. Kielpinski, D. E. Pritchard, and W. Ketterle, “Cooling bose-einstein condensates below 500 picokelvin,” *Science* **301**, 1513–1515 (2003), <https://www.science.org/doi/pdf/10.1126/science.1088827>.
- [53] David C. Aveline, Jason R. Williams, Ethan R. Elliott, Chelsea Dutenhoffer, James R. Kellogg, James M. Kohel, Norman E. Lay, Kamal Oudrhiri, Robert F. Shotwell, Nan Yu, and Robert J. Thompson, “Observation of bose-einstein condensates in an earth-orbiting research lab,” *Nature* **582**, 193–197 (2020).
- [54] Ryan Olf, Fang Fang, G. Edward Marti, Andrew MacRae, and Dan M. Stamper-Kurn, “Thermometry and cooling of a bose gas to 0.02 times the condensation temperature,” *Nature Physics* **11**, 720–723 (2015).
- [55] Quentin Bouton, Jens Nettersheim, Daniel Adam, Felix Schmidt, Daniel Mayer, Tobias Lausch, Eberhard Tieemann, and Artur Widera, “Single-atom quantum probes for ultracold gases boosted by nonequilibrium spin dynamics,” *Phys. Rev. X* **10**, 011018 (2020).
- [56] L. Wacker, N. B. Jørgensen, D. Birkmose, R. Horchani, W. Ertmer, C. Klempt, N. Winter, J. Sherson, and J. J. Arlt, “Tunable dual-species bose-einstein condensates of ^{39}K and ^{87}Rb ,” *Phys. Rev. A* **92**, 053602 (2015).
- [57] Stefan Schmid, Arne Härter, and Johannes Hecker Denschlag, “Dynamics of a cold trapped ion in a bose-einstein condensate,” *Phys. Rev. Lett.* **105**, 133202 (2010).
- [58] Felix Schmidt, Daniel Mayer, Quentin Bouton, Daniel Adam, Tobias Lausch, Nicolas Spethmann, and Artur Widera, “Quantum spin dynamics of individual neutral impurities coupled to a bose-einstein condensate,” *Phys. Rev. Lett.* **121**, 130403 (2018).
- [59] Marko Cetina, Michael Jag, Rianne S. Lous, Isabella Fritsche, Jook T. M. Walraven, Rudolf Grimm, Jesper Levinsen, Meera M. Parish, Richard Schmidt, Michael Knap, and Eugene Demler, “Ultrafast many-body interferometry of impurities coupled to a fermi sea,” *Science* **354**, 96–99 (2016), <https://www.science.org/doi/pdf/10.1126/science.aaf5134>.

- [60] Petr O. Fedichev and Uwe R. Fischer, “Observer dependence for the phonon content of the sound field living on the effective curved space-time background of a bose-einstein condensate,” *Phys. Rev. D* **69**, 064021 (2004).
- [61] Zehua Tian and Jiangfeng Du, “Probing low-energy lorentz violation from high-energy modified dispersion in dipolar bose-einstein condensates,” *Phys. Rev. D* **103**, 085014 (2021).
- [62] Ph. Courteille, R. S. Freeland, D. J. Heinzen, F. A. van Abeelen, and B. J. Verhaar, “Observation of a feshbach resonance in cold atom scattering,” *Phys. Rev. Lett.* **81**, 69–72 (1998).
- [63] S. Inouye, M. R. Andrews, J. Stenger, H. J. Miesner, D. M. Stamper-Kurn, and W. Ketterle, “Observation of feshbach resonances in a bose-einstein condensate,” *Nature* **392**, 151–154 (1998).
- [64] M. Zaccanti, C. D’Errico, F. Ferlaino, G. Roati, M. Inguscio, and G. Modugno, “Control of the interaction in a fermi-bose mixture,” *Phys. Rev. A* **74**, 041605 (2006).
- [65] Andrea Simoni, Matteo Zaccanti, Chiara D’Errico, Marco Fattori, Giacomo Roati, Massimo Inguscio, and Giovanni Modugno, “Near-threshold model for ultracold krb dimers from interisotope feshbach spectroscopy,” *Phys. Rev. A* **77**, 052705 (2008).
- [66] Cheng Chin, Rudolf Grimm, Paul Julienne, and Eite Tiesinga, “Feshbach resonances in ultracold gases,” *Rev. Mod. Phys.* **82**, 1225–1286 (2010).

Supplementary Material

I. THE MODEL

Our detector model is inspired by the atomic quantum dot ideal originally introduced in Refs. [26, 27, 60]. It consists of an impurity which can be considered as a two-level (1 and 2) atom, and is immersed in a one-dimensional atomic BEC at very low temperature. The impurity is assumed to be illuminated by a monochromatic external electromagnetic field at the frequency ω_L which is close to resonance with the $1 \rightarrow 2$ transition $\omega_L \simeq \omega_{21}$, with a (real and positive) time-dependent Rabi frequency $\omega_0(t)$. This kind of model has been fruitfully applied in various fields, such as investigating Casimir forces and quantum friction from Ginzburg radiation [46], zero-point excitation of a circularly moving detector [8], and Lorentz-invariance-violation-induced physics [9, 61].

Specifically, the Hamiltonian of the whole system is of the form

$$H(t) = H_B + H_A(t) = \int dk \omega_k \hat{b}_k^\dagger \hat{b}_k + \omega_{21} |2\rangle\langle 2| - \left(\frac{\omega_0(t)}{2} e^{-i\omega_L t} |2\rangle\langle 1| + \text{H.c.} \right) + \sum_s g_s \hat{\rho}(x_A(t)) |s\rangle\langle s|, \quad (\text{S1})$$

where the last term is the collisional coupling between the impurity and Bose gas. $\hat{\rho}(x_A) = \hat{\psi}^\dagger(x_A) \hat{\psi}(x_A)$ denotes the field density operator of the atomic Bose gas, and $x_A(t)$ is the time-dependent impurity position. g_s are the interaction constant between the impurity in $s = 1, 2$ state and the condensate. In the rotating frame, the detector's Hamiltonian including its interaction with the Bose gas can be rewritten as

$$H_A(t) = \omega_{21} |2\rangle\langle 2| - \frac{1}{2} \omega_L (|2\rangle\langle 2| - |1\rangle\langle 1|) - \frac{1}{2} \omega_0(t) (|2\rangle\langle 1| + |1\rangle\langle 2|) + \sum_s g_s \hat{\rho}(x_A(t)) |s\rangle\langle s|. \quad (\text{S2})$$

Then, using the rotated $|g, e\rangle = (1/\sqrt{2})(|1\rangle \pm |2\rangle)$ basis and defining $g_\pm = \frac{1}{2}(g_1 \pm g_2)$, we can further rewrite the Hamiltonian (S2) as

$$H_A(t) = \frac{\omega_0(t)}{2} \sigma_z + \frac{\delta}{2} \sigma_x + \hat{\rho}(x_A(t)) [g_+ + g_- \sigma_x], \quad (\text{S3})$$

where σ_z and σ_x are the conventional Pauli matrices, and $\delta = \omega_L - \omega_{21}$ is the detuning. In this rotated basis, the time-dependent Rabi frequency $\omega_0(t)$ determines the splitting between the $|g\rangle, |e\rangle$ states, while the detuning δ gives a coupling term.

Let us note the last term of the above Hamiltonian (S3) denotes the interaction between the impurity and Bose gas. This interaction contains two terms: the first one proportional to g_+ is similar to the reminiscent coupling of a charged particle to an electric field, while the other resembles a standard electric-dipole coupling mediated by a coupling constant g_- . By suitably choosing the internal atomic states and properly tuning the interaction constants (e.g., via Feshbach resonances [62, 63]), the first term could be cancelled as a result of $g_+ = 0$ [64–66], behaving like the analog charge neutrality. Furthermore, the atomic density operator $\hat{\rho}(x)$, as shown above, can be split into its average value ρ_0 and small fluctuations $\delta\hat{\rho}(x)$ in (14). With the suitable detuning δ between driving frequency and the impurity's internal level space, one can exactly compensate the coupling to the average density, $\delta/2 + g_- \rho_0 = 0$ [8, 46]. Under all these assumptions, the impurity's Hamiltonian including the interaction with the condensate can finally be written as

$$H_A(t) = \frac{\omega_0(t)}{2} \sigma_z + g_- \sigma_x \delta\hat{\rho}(x_A). \quad (\text{S4})$$

The coupling of the impurity to the condensate in the Hamiltonian (S4) has the analogous form $g_- \sigma_x \delta\hat{\rho}(x_A)$ of a two-level atom dipole coupled to the one dimensional quantum scalar field at its position x_A . In the interaction picture with respect to the analogue quantum field, we can find the Hamiltonian for the whole system then can be written as

$$H(t) = \frac{\omega_0(t)}{2} \sigma_z + g_- \sigma_x \delta\hat{\rho}(x_A, t). \quad (\text{S5})$$

Note here that $\delta\hat{\rho}(x_A, t)$ denotes the density fluctuation operator in the interaction picture.

II. CORRELATION FUNCTION OF THE DENSITY FLUCTUATIONS

Let us present the associate expression for the correlation function of the density fluctuations. It is given by

$$\begin{aligned}
\langle 0 | \delta \hat{\rho}(t, x) \delta \hat{\rho}(t', x') | 0 \rangle &= \frac{\rho_0}{(2\pi)^2} \int \int dk dk' (u_k + v_k)(u_{k'} + v_{k'}) \langle 0 | [\hat{b}_k(t) e^{ikx} + \text{h.c.}] [\hat{b}_{k'}(t') e^{ik'x'} + \text{h.c.}] | 0 \rangle \quad (\text{S6}) \\
&= \frac{\rho_0}{(2\pi)^2} \int \int dk dk' (u_k + v_k)(u_{k'} + v_{k'}) e^{-i\omega_k t + i\omega_{k'} t'} e^{ikx - ik'x'} (2\pi) \delta(k - k') \\
&= \frac{\rho_0}{2\pi} \int dk (u_k + v_k)^2 e^{-i\omega_k(t-t')} e^{ik(x-x')} \\
&= \frac{\rho_0}{2\pi} \int dk \frac{k^2/2m}{\omega_k} e^{-i\omega_k \Delta t} e^{ik \Delta x} \\
&= -\frac{\rho_0}{4\pi m c_0} \frac{1}{[\Delta x - (c_0 \Delta t - i\epsilon)]^2}, \quad (\text{S7})
\end{aligned}$$

where $\Delta x = x - x'$ and $\Delta t = t - t'$ have been defined. Besides, in the last integral we have assumed the long wavelength (phononic) regime, i.e., neglecting the quantum pressure term $\sim \nabla^2 \delta \rho$, and thus we have $\omega_k \approx c_0 k$, as done in Refs. [6, 10].